ResearchGate

See discussions, stats, and author profiles for this publication at: https://www.researchgate.net/publication/222810963

Predicting the acoustical radiation of finite size multi-layered structures by applying spatial windowing on infinite structures

Article *in* Journal of Sound and Vibration · August 2001

DOI: 10.1006/jsvi.2001.3592

CITATIONS
98

READS
137

3 authors, including:

Laurent Gagliardini
PSA Peugeot Citroen
71 PUBLICATIONS **512** CITATIONS

SEE PROFILE

All content following this page was uploaded by Laurent Gagliardini on 18 October 2016.

The user has requested enhancement of the downloaded file.

Predicting the acoustical behavior of finite size structures by applying spatial windowing on infinite structures

M. Villot, C. Guigou and L. Gagliardini[1]

C.S.T.B.
Noise and Vibration Division
24, Rue Joseph Fourier
38400 Saint Martin d'Hères, France

[1]Currently working at
P.S.A. Peugeot-Citroën
18 Rue des Fauvelles, B.P. 16
92256 La Garenne-Colombes Cedex

Number of pages: XX

Number of Tables: XX

Number of Figures: XX

Number of Manuscript Copies:

Running Headline:

Correspondence: M. Villot

C.S.T.B.

Noise and Vibration Division

24, Rue Joseph Fourier

38400 Saint Martin d'Hères, France

email : villot@cstb.fr

ABSTRACT

A new technique based on a spatial windowing is presented in order to take the finite size of a plane structure into account without any modal calculations. This technique allows to obtain prediction results much closer to experimental measurements than the classical wave approach applied to infinite structure. In the first part, the principle of the technique is given as well as the derivation of the modified sound radiation efficiency. In the second part, some predicted results including the sound transmission index of an aluminum plate and a double leaf window, as well as the radiation efficiency of a metal plate mechanically excited, are given and compared to experimental results in order to validate the spatial windowing technique. The effect of the structure size on both its sound transmission (acoustical excitation) and its sound radiation (mechanical excitation) is also discussed.

1. INTRODUCTION

The wave approach is generally used to study the sound transmission through planar structures ; it consists of calculating the sound reduction index of an infinite plane structure excited by a single or random (diffuse field) incident plane waves. This approach has the advantage of clearly showing the dominant physical phenomena involved, such as the critical frequency for single leaf partitions or the resonance frequency for double leaf partitions (see for example Chapter 4 in reference [1]) ; it greatly simplifies the calculation of sound transmission through multilayered structures by means of the transfer matrix technique as developed by Munjal [2] and always corresponds to relatively short computation time. However, the calculated results are often quite far from experimental curves : the calculated sound reduction index associated with a single leaf panel for example shows important discrepancies especially at low frequencies. In the past, one way to reduce the difference between the results from the wave approach theory and experiments, has been to reduce the diffuseness of the acoustic field incident on the infinite structure [3-5]. This of course strongly influence the results (as will be seen in Section 3) ; however, the general behavior is not much improved at low frequencies. It should also be noticed that the modal behavior displayed by experimental measurements at low frequencies are not of first importance since it varies with the structure tested, its size and boundary conditions (which are usually unknown). Indeed, the general tendencies in the low frequency range are more of interest.

The wave approach also gives poor results (compared to experimental ones) when calculating the sound radiated by a planar structure mechanically excited by a point force ; indeed, the radiation efficiency of an infinite plate mechanically excited below its critical frequency is too low.

In this paper, a new technique based on a spatial windowing is presented, in order to take the finite size of the plane structure into account without any modal calculations. It allows to obtain

prediction results much closer to experimental measurements than the classical wave approach applied to infinite structure. In a first section, the principle of the technique is given as well as the derivation of the modified radiation efficiencies. In a second section, some calculated results including the sound reduction index of an aluminum plate and a double leaf window as well as the radiation efficiency of a metal plate mechanically excited are given and compared to experimental results in order to validate the spatial windowing technique. The effect of the structure size on both its sound transmission (case of acoustical excitation) and its sound radiation (case of mechanical excitation) is also discussed.

2. THE SPATIAL WINDOWING TECHNIQUE

2.1. Principle

The principle of the technique consists of spatially windowing the excitation pressure field (case of acoustical excitation), calculating the resulting vibration velocity field of the infinite structure and spatially windowing this vibration field before calculating the radiated field. In case of mechanical excitation, only the spatial windowing of the vibration velocity field is performed before calculating the radiated field.

In this section, a qualitative explanation of the spatial windowing technique is given in the wavenumber domain for a 1-dimensional structure in order to better understand the derivation developed in Section 2.2.

2.1.1. Acoustical Excitation

Figure 3(a) shows an infinite plate acoustically excited by an oblique (angle θ) incident plane wave of amplitude A. In the wavenumber domain and at a given frequency ω, the excitation pressure field is then represented by a delta Dirac function as depicted in Figure 3(b). A single wavenumber $k_x=k_a\sin\theta$ is represented in the excitation spectrum and a single wave with that particular wavenumber will propagate in the infinite structure. Note that k_a represents the wavenumber in the surrounding fluid (air) and is defined by $k_a=\omega/c_a$ (with c_a is the speed of sound in air).

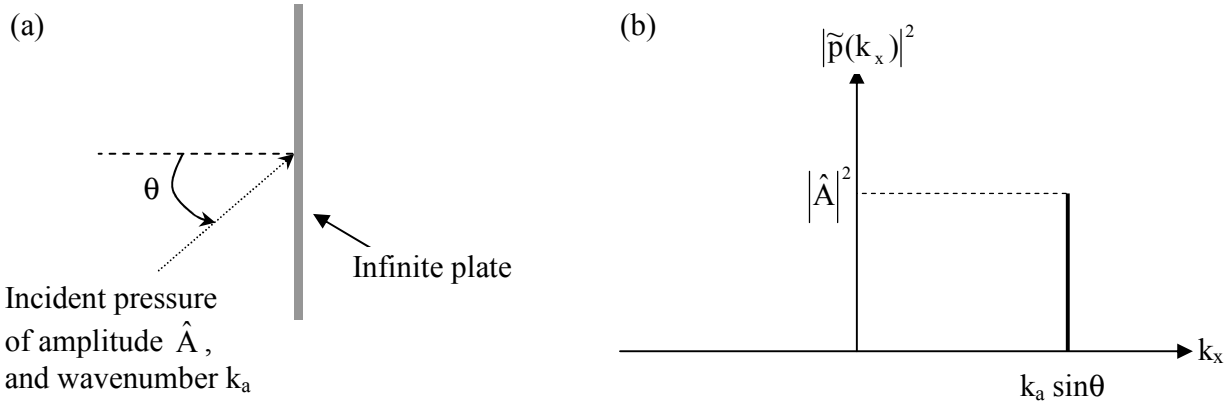

Figure 3: (a) Acoustically excited infinite plate
and (b) associated incident pressure wavenumber spectrum.

On the other hand, in the case of a finite size system, it can be considered that the incident pressure wave goes through a diaphragm (of length a) before impinging on the infinite structure as shown in figure 4(a). In that case, the incident pressure field wavenumber spectrum, as seen in Figure 4(b), is spread over the entire wavenumber domain. It should be noticed that even if the excitation frequency is smaller than the plate critical frequency (i.e., the flexural wavenumber k_f greater than the acoustical wavenumber k_a), the windowed pressure field will not only generate a forced travelling wave (k_x close

to $k_a \sin\theta$) but also a free travelling flexural wave (k_x close to k_f) since there is excitation energy around k_f.

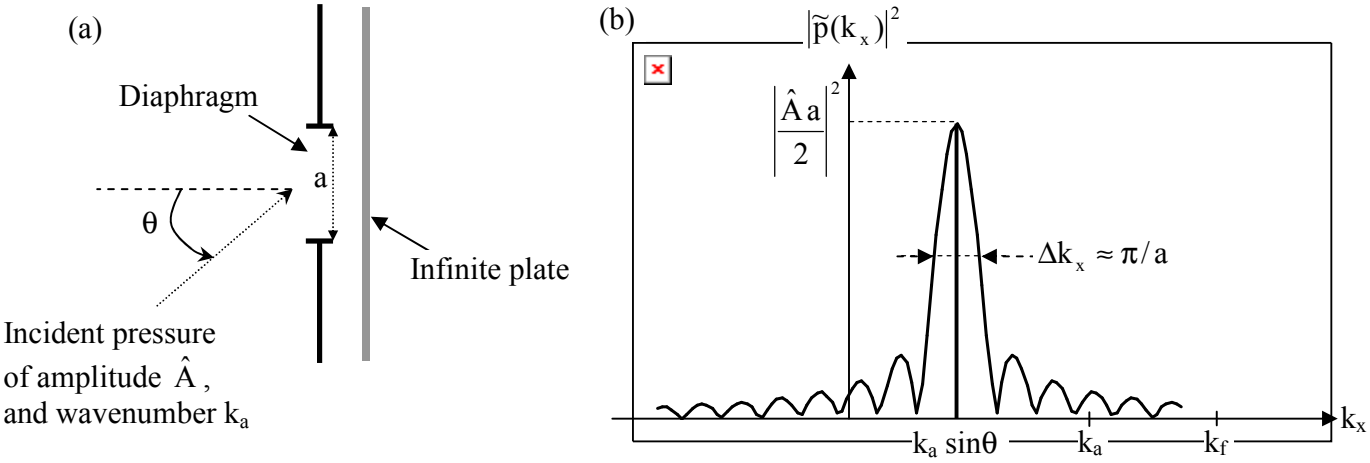

Figure 4: (a) Spatial windowing of acoustic incident field exciting an infinite plate and (b) associated incident pressure wavenumber spectrum.

2.1.2. Structural Excitation

A structural excitation distributed over the small length *l* of the structure, as shown in Figure 5(a) is now considered. This type of mechanical load can be decomposed into an infinite number of travelling normal stress waves as shown in figure 5(b). In this case, no windowing is required at the excitation stage.

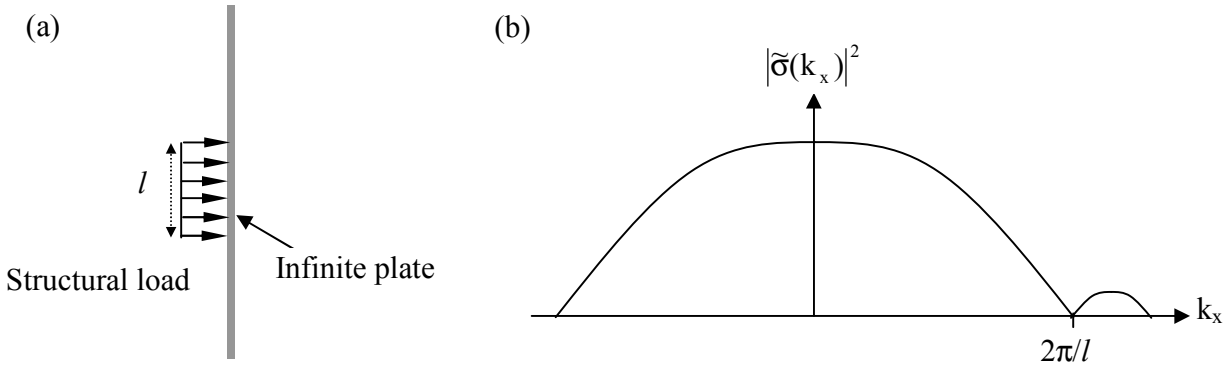

Figure 5: (a) Structural excitation on an infinite plate
and (b) associated stress wavenumber spectrum.

2.1.3. Radiation

Figure 6(a) shows in the spatial domain (real space) a structural plane wave (wavenumber k_p) travelling along an infinite structure. The velocity wavenumber spectrum includes in that case a single component at $k_x=k_p$ as presented in Figure 6(b). Only wavenumbers smaller than the wavenumber in the surrounding fluid k_a ($k_x<k_a$), i.e. corresponding to a supersonic wave, participates to sound radiation ; therefore, in the case presented in Figure 6(b), sound radiation will occur (since $k_p<k_a$). On the other hand, if $k_p>k_a$, no sound will be radiated in the far-field.

Considering that only a length a of the structure participates in the sound radiation (see Figure 7(a)), leads to the velocity wavenumber spectrum shown in Figure 7(b). The energy is once again spread over the whole wavenumber domain. In this case, if the structural wavenumber k_p is larger than k_a (as shown in figure 7(b)), wavenumber components associated to sound radiation (i.e., $k_x<k_a$) are present in the velocity wavenumber spectrum, and the radiation efficiency will be small but not zero.

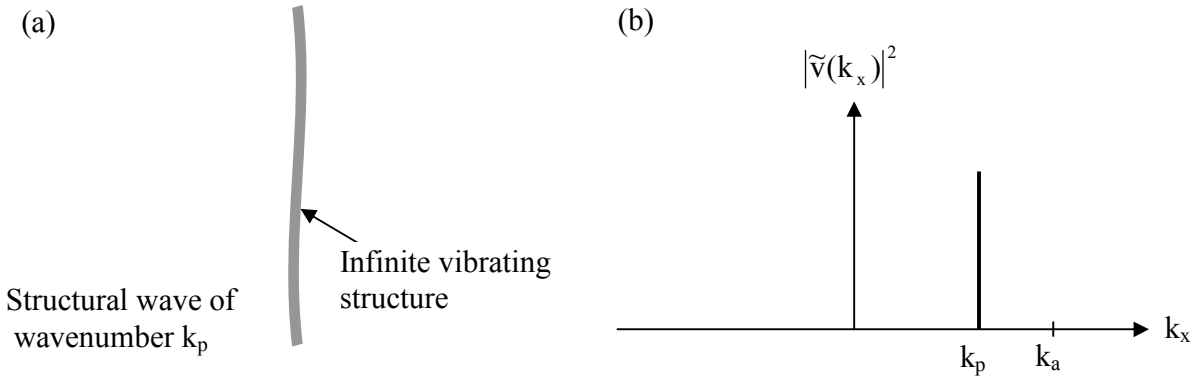

Figure 6: (a) Structural wave propagating in an infinite structure and (b) associated velocity wavenumber spectrum.

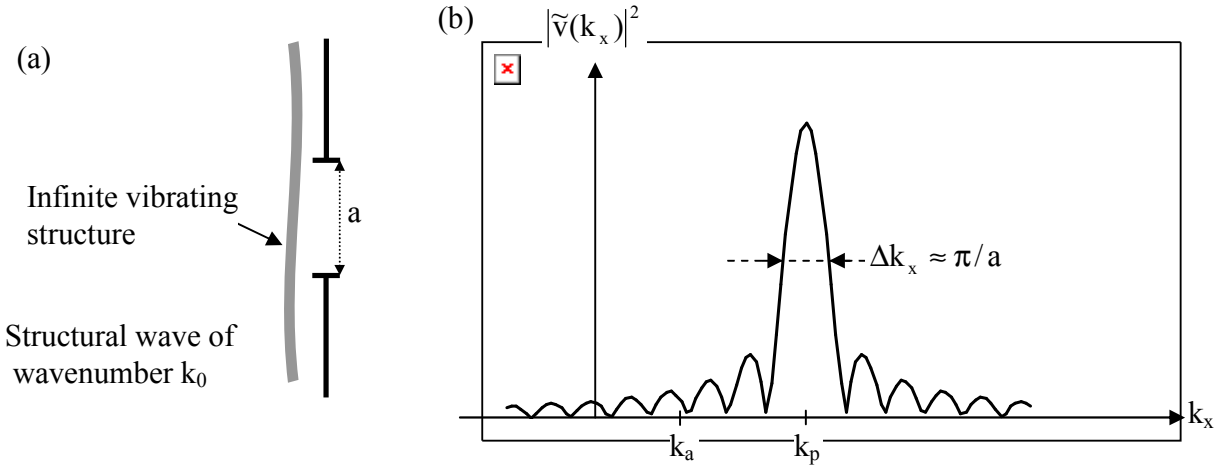

Figure 7: (a) Spatial windowing of a structural wave propagating in an infinite structure and (b) associated velocity wavenumber spectrum.

2.2. Radiation efficiency associated with spatial windowing

A structural wave of wave number k_p is assumed to propagate on an infinite two-dimensional structure in the direction ψ; the wave number components k_{px}, k_{py} can be written as :

$$\begin{cases} k_{px} = k_p \cos\psi \\ k_{py} = k_p \sin\psi \end{cases} \tag{1}$$

The time dependence of the different fields is assumed to be in the form $e^{i\omega t}$ and will be omitted for conciseness. The velocity field in the spatial domain can then be written as

$$v(x,y) = \hat{v}_s \; e^{-ik_{px}x} \; e^{-ik_{py}y} \tag{2}$$

Let us consider that only a surface S (of length L_x and width L_y) of the structure participates in the sound radiation ; the velocity field in the wavenumber domain is then defined by taking the spatial Fourier transform

$$\begin{aligned} \tilde{v}(k_x,k_y) &= \hat{v}_s \int_{-L_x/2}^{L_x/2} \int_{-L_y/2}^{L_y/2} e^{-ik_{px}x} \; e^{-ik_{py}y} e^{ik_x x} \; e^{ik_y y} \; dx\, dy \\ &= \hat{v}_s \; L_x L_y \; \frac{\sin\left((k_x - k_p\cos\psi)L_x/2\right)}{\left((k_x - k_p\cos\psi)L_x/2\right)} \cdot \frac{\sin\left((k_y - k_p\sin\psi)L_y/2\right)}{\left((k_y - k_p\sin\psi)L_y/2\right)} \end{aligned} \tag{3}$$

The radiated power calculated from the wavenumber spectrum of the velocity field can be expressed by [1]

$$\Pi(k_p,\psi) = \frac{\rho_a c_a}{8\pi^2} \int_0^{k_a} \int_0^{2\pi} \frac{\left|\tilde{v}(k_r\cos\phi, k_r\sin\phi)\right|^2}{\sqrt{k_a^2 - k_r^2}} \, k_a \, k_r \, d\phi \, dk_r \tag{4}$$

where k_a is the wavenumber in the air (see above) and ρ_a is the air density (the expression $\rho_a c_a \frac{k_a}{\sqrt{k_a^2 - k_r^2}}$ in equation (4) corresponds to the classical fluid wave impedance). As shown in Figure

8, only wavenumber components of the velocity wavenumber spectrum inside the circle of radius k_a participate to the sound radiated power.

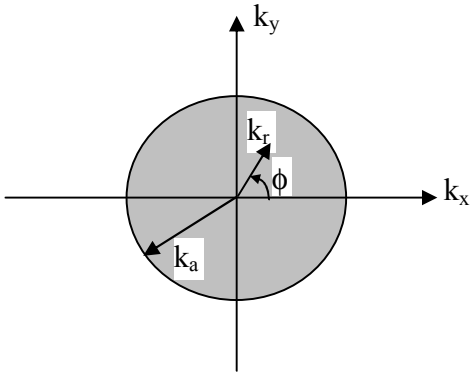

Figure 8: Wavenumber components contributing to sound radiated power

The radiation efficiency can be calculated from

$$\sigma(k_p,\psi)=\frac{\Pi(k_p,\psi)}{\rho_a c_a S\langle v^2\rangle} \tag{5}$$

where $\langle v^2\rangle$ is the mean squared velocity defined as

$$\langle v^2\rangle=\frac{1}{2S}\int_S |v(x,y)|^2 dS=\frac{|\hat{v}_s|^2}{2} \tag{6}$$

Using Equations (3), (4) and (6) in (5) leads to the following expression of the radiation efficiency for a traveling structural wave

$$\sigma(k_p,\psi)=\frac{S}{\pi^2}\int_0^{k_a}\int_0^{2\pi}\frac{1-\cos((k_r\cos\phi-k_p\cos\psi)L_x)}{\left[(k_r\cos\phi-k_p\cos\psi)L_x\right]^2}\cdot\frac{1-\cos((k_r\sin\phi-k_p\sin\psi)L_y)}{\left[(k_r\sin\phi-k_p\sin\psi)L_y\right]^2}\frac{k_a k_r}{\sqrt{k_a^2-k_r^2}}d\phi\,dk_r \tag{7}$$

In order to get a radiation efficiency independent of the travelling direction ψ, a structural diffuse field radiation efficiency $<\sigma(k_p)>_\psi$ can then be rewritten as the triple integral

$$<\sigma(k_p)>_\psi = \frac{S}{2\pi^3}\int_0^{2\pi}\int_0^{k_a}\int_0^{2\pi} \frac{1-\cos(\left(k_r\cos\phi - k_p\cos\psi\right)L_x)}{\left[\left(k_r\cos\phi - k_p\cos\psi\right)L_x\right]^2}\cdot\frac{1-\cos(\left(k_r\sin\phi - k_p\cos\psi\right)L_y)}{\left[\left(k_r\sin\phi - k_p\cos\psi\right)L_y\right]^2} \times \frac{k_a\,k_r}{\sqrt{k_a^2-k_r^2}}\,d\phi\,dk_r\,d\psi \quad (8)$$

In order to show $<\sigma(k_p)>_\psi$ as a function of frequency, the example of the bending wave number k_p of a thin plate (proportional to $\sqrt{\omega}$) is chosen. The surface S of the radiating part of the plate is of length L_x=1.4 m and width L_y=1.1 m; the plate material properties (gypsum board) are given in Table I. Figure 9 presents the radiation efficiency obtained after integrating Equation (8). It can be seen that, below the critical frequency of the plate (marked f_c in Figure 9), the radiation efficiency obtained with the spatial windowing technique is small but not null (the radiation efficiency for an infinite structure on which travels a propagating bending wave would be zero below the critical frequency). As expected, the radiation efficiency tends to unity for frequencies higher than the critical frequency.

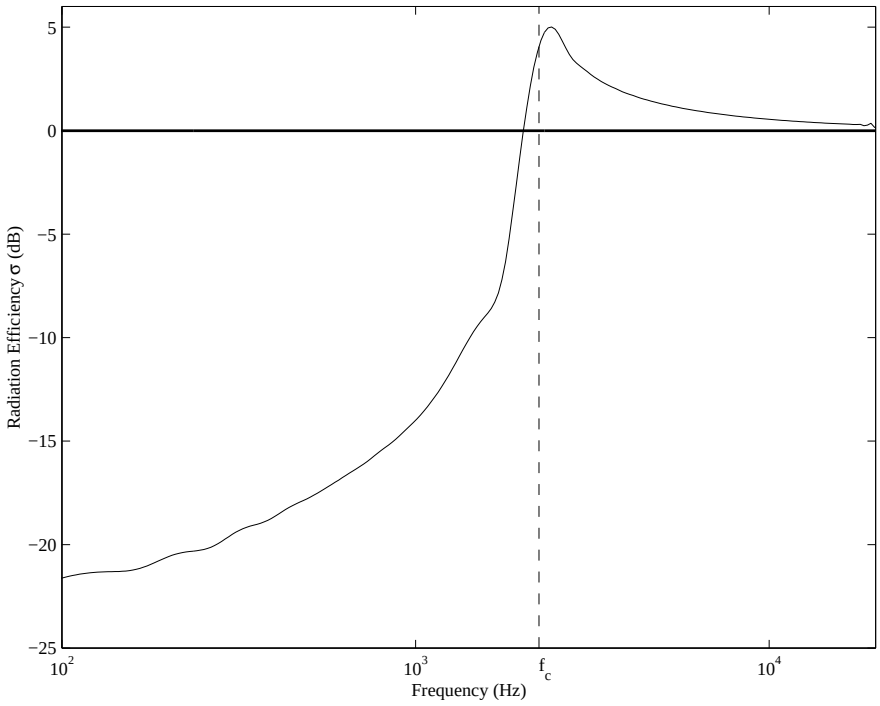

Figure 9: Radiation efficiency $<\sigma(k_p)>_\psi$ after spatial windowing for a system in bending.

2.3. Applying spatial windowing to sound transmission

2.3.1.Radiation efficiency

For an incident acoustic plane wave, the wave number k_p is related to the incident angle θ by $k_p = k_a \sin\theta$. In this case, the radiation efficiency for an infinite system (no spatial windowing) is given by

$$\sigma_{inf} = 1/\cos\theta \tag{9}$$

Figure 10 shows the diffuse field radiation efficiency $<\sigma(k_a \sin\theta)>_\psi$ associated with the spatial filtering of the infinite structure (Equation (8)) for an acoustic wave excitation as a function of frequency and incidence angle. In this example, the surface S of the structure participating to the sound radiation is of length L_x=1.4 m and width L_y=1.1 m. Figure 11 presents the radiation efficiency for two different frequencies of the spatially windowed system as well as that of the infinite system (Equation (9)). Two regions can be observed in Figure 10 :

1. For frequencies below about 300 Hz (about λ>L/2 with L characteristic length of the finite structure), the radiation efficiency of the finite structure (using spatial filtering) is lower than that of the infinite system for any angle of incidence (frequency f_1 in Figure 11),

2. At higher frequencies, the radiation efficiency of the finite structure (using spatial filtering) is lower than that of the infinite one only above a certain incidence angle (frequency f_2 in Figure 11).

Therefore at low frequency, the radiation from finite structure will always be less than that of the associated infinite structure.

Note that $<\sigma(k_a \sin\theta)>_\psi$ do not depend on the structure considered but only on the size of the rectangular window ; the radiation efficiencies corresponding to typical dimensions of walls, glazing.. can therefore be pre-calculated.

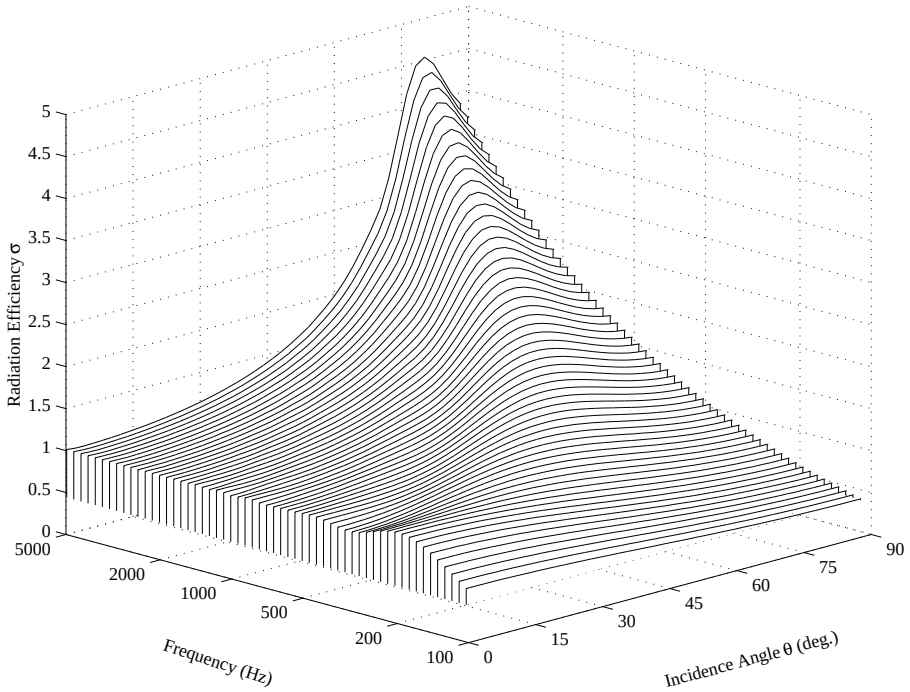

Figure 10: Radiation efficiency of an infinite structure after applying the spatial windowing technique.

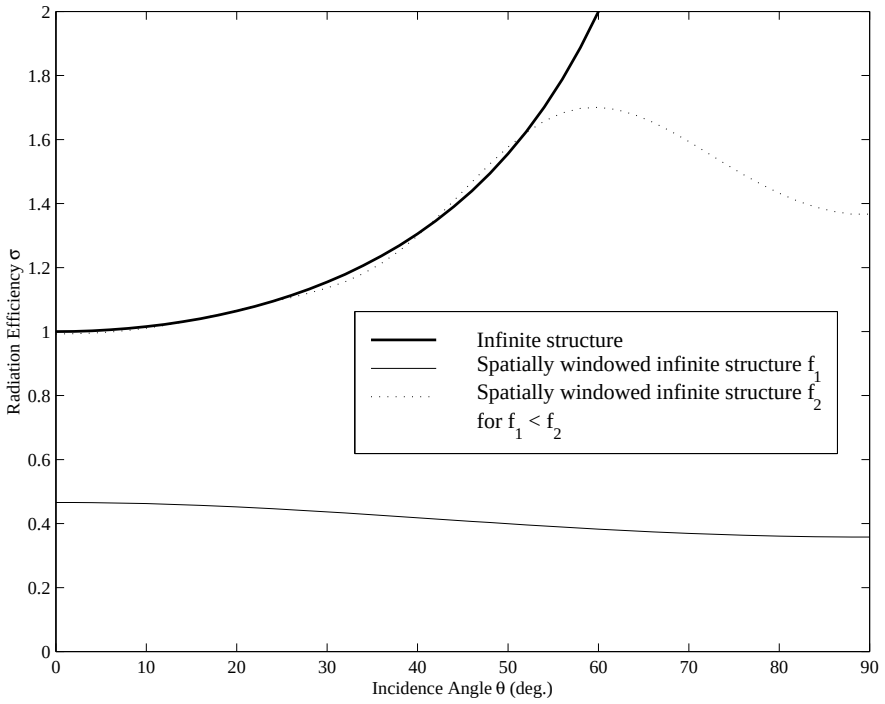

Figure 11: Radiation efficiency of an infinite structure before and after applying the spatial windowing technique.

2.3.2.Sound transmission

The spatial windowing is now directly applied to the problem of sound transmission through a structure. The sound reduction index associated with the infinite structure is assumed to be known, i.e. calculated using the transfer matrix method as described in [2] and [5]. It is denoted by $\tau_{inf}(\theta)$ where θ is the incidence angle of the plane wave excitation of amplitude $\hat{p}_i$, and is expressed as the ratio of the transmitted sound intensity to the incident intensity, i.e.

$$\tau_{inf}(\theta) = \frac{I_{inf\_trans}}{I_{inf\_inc}} = \frac{\rho_a c_a}{2} \frac{\left|\hat{v}_s\right|^2}{\cos\theta} \frac{1}{I_{inf\_inc}} \tag{10}$$

where $\rho_a c_a / \cos\theta$ represents the wave radiation impedance.

Applying first the spatial windowing to the radiation process, a new sound transmission index can be defined by

$$\tau_{1\_finite}(\theta,\psi) = \frac{\Pi_{finite\_trans}}{I_{inf\_inc}\, S} \tag{11}$$

with Π_{finite_trans} the transmitted power given by Equation (4) where the velocity field of the infinite structure has been spatially windowed. Using the derivations presented in Section 2.2, Equation (11) can be rewritten as

$$\tau_{1\_finite}(\theta,\psi) = \frac{I_{inf\_trans}}{I_{inf\_inc}} \frac{\Pi_{finite\_trans}}{I_{inf\_trans} S} = \tau_{inf}(\theta) \frac{\Pi_{finite\_trans}}{S \frac{\rho_a c_a}{2} \frac{|\hat{v}_s|^2}{\cos\theta}} = \tau_{inf}(\theta)\ \sigma(k_a \sin\theta, \psi) \cos\theta \tag{12}$$

where Π_{finite_trans} is given by equation (5) and (6).

The same process can be applied to obtain the effect of spatially windowing the incident pressure field $p_i(x,y) = \hat{p}_i e^{-ik_a \sin\theta\cos\psi.x} e^{-ik_a \sin\theta\sin\psi.y}$; a correcting factor $\tau_{2\_finite}(\theta,\psi)$ can be defined as

$$\tau_{finite}(\theta,\psi) = \tau_{2\_finite}(\theta,\psi).\tau_{1\_finite}(\theta,\psi) \tag{13}$$

with $\tau_{finite}(\theta,\psi)$ the transmission factor resulting from windowing both the excitation pressure field and the radiated field. $\tau_{2\_finite}(\theta,\psi)$ can be expressed as :

$$\tau_{2\_finite}(\theta,\psi) = \frac{\Pi_{finite\_inc}}{I_{inf\_inc} S} = \frac{\Pi_{finite\_inc}}{\frac{|\hat{p}_i|^2 \cos\theta}{2\rho_a c_a} S} \tag{14}$$

The particle velocity component normal to the x,y plane of the not windowed incident field can be expressed in the real space as

$$v_{i,n}(x,y) = p_i(x,y).\frac{\cos\theta}{\rho_a c_a} \tag{15}$$

The wave number spectrum of the windowed incident particle velocity $\tilde{v}_{i,n}(k_x, k_y)$ can be calculated using equation (3), by replacing $\hat{v}_s$ by $\hat{p}_i.\frac{\cos\theta}{\rho_a c_a}$:

$$\tilde{v}_{i,n}(k_x,k_y)=\hat{p}_i.\frac{\cos\theta}{\rho_a c_a}L_xL_y\,\frac{\sin\left((k_x-k_a\sin\theta.\cos\psi)L_x/2\right)}{\left((k_x-k_a\sin\theta.\cos\psi)L_x/2\right)}.\frac{\sin\left((k_y-k_a\sin\theta.\sin\psi)L_y/2\right)}{\left((k_y-k_a\sin\theta.\sin\psi)L_y/2\right)} \qquad (16)$$

and the incident power Π_{finite_inc} can then be obtained by replacing $\tilde{v}(k_r\cos\phi,k_r\sin\phi)$ by $\tilde{v}_{i,n}(k_r\cos\phi,k_r\sin\phi)$ in equation (4). Using equation (5) and (6), Π_{finite_inc} can finally be expressed as

$$\Pi_{finite\_inc}(\theta,\psi)=\rho_a c_a S.\sigma(k_a\sin\theta,\psi).\frac{\left|\hat{v}_{i,n}\right|^2}{2}=\frac{\left|\hat{p}_i\right|^2\cos^2\theta}{2\rho_a c_a}S.\sigma(k_a\sin\theta,\psi) \qquad (17)$$

and equation (14) becomes

$$\tau_{2\_finite}(\theta,\psi)=\cos\theta\ \sigma(k_a\sin\theta,\psi) \qquad (18)$$

The transmission index associated with the finite structure after applying the spatial windowing technique is finally given by

$$\tau_{finite}(\theta,\psi)=\tau_{2\_finite}(\theta,\psi)\,\tau_{1\_finite}(\theta,\psi)=\tau_{inf}(\theta)\,\sigma(k_a\sin\theta,\psi)\cos\theta\ \sigma(k_a\sin\theta,\psi)\cos\theta \qquad (19)$$

Therefore, for an acoustic excitation field, the infinite system is affected twice by the modification of the radiation efficiency (as explained in Section 2) : both the incident field and the radiation are modified.

2.4. Applying spatial windowing to sound radiation from structurally excited structure

2.4.1. Radiation efficiency

The structure is now assumed to be subjected to a structural excitation (force). Therefore, an infinite number of propagating waves, generated by an infinite number of traveling normal stress waves as explained in section 2.1.2, propagate in the structure. The velocity field $\tilde{v}_{inf}(k_x,k_y)$ in the wave number domain for the infinite structure is assumed to be known, i.e. calculated using the transfer matrix method (at one of the two free surfaces of the multilayered structure considered). The velocity field in the wavenumber domain of the spatially windowed structure (surface S of length L_x and width L_y) can be expressed as a convolution multiplication, i.e.,

$$\tilde{v}_{finite}(k_x,k_y)=\tilde{v}_{inf}(k_x,k_y)\otimes\left[L_xL_y\,\frac{\sin(k_xL_x/2)}{(k_xL_x/2)}.\frac{\sin(k_yL_y/2)}{(k_yL_y/2)}\right] \tag{20}$$

where $\otimes$ denotes the convolution multiplication. This convolution is numerically calculated. The radiated power for the spatially windowed structure is then given by (see Equation (4))

$$\Pi_{finite}(\omega)=\frac{\rho_a c_a}{8\pi^2}\int_0^{k_a}\int_0^{2\pi}\frac{\left|\tilde{v}_{finite}(k_r\cos\phi,k_r\sin\phi)\right|^2}{\sqrt{k_a^2-k_r^2}}\,k_a\,k_r\,d\phi\,dk_r \tag{21}$$

The mean squared velocity associated with the spatially windowed structure $\langle v^2\rangle_{finite}$ can be expressed according to Parseval's theorem

$$\langle v^2\rangle_{finite}=\frac{1}{4\pi^2}\frac{1}{2S}\int_{-\infty}^{+\infty}\int_{-\infty}^{+\infty}\left|\tilde{v}_{finite}(k_x,k_y)\right|^2 dk_x\,dk_y \tag{22}$$

and the radiation efficiency is finally deduced from

$$\sigma_{finite}(\omega)=\frac{\Pi_{finite}(\omega)}{\rho_a c_a S\langle v^2\rangle_{finite}} \tag{23}$$

The same structure with the same dimensions as in section 2.2 is now considered to illustrate the previous derivations. In the case of the spatially windowed structure, the excitation force is taken to be located at the center of the plate. The radiation efficiency for the infinite and spatially windowed structure is shown is Figure 12. This time, for the infinite system and at frequencies much lower than the critical frequency (marked f_c in figure 12), the radiation efficiency is not null due to the fact that supersonic waves generated by supersonic stress waves exist (see section 2.1.2) and participate to the sound radiation. By spatially windowing the system, the radiation efficiency is increased for frequencies much lower than the critical frequency, since more supersonic waves participate to the sound radiation as explained in section 2.1.3. As expected, for frequencies close to and larger than the critical frequency, spatially windowing has no impact on the radiation efficiency.

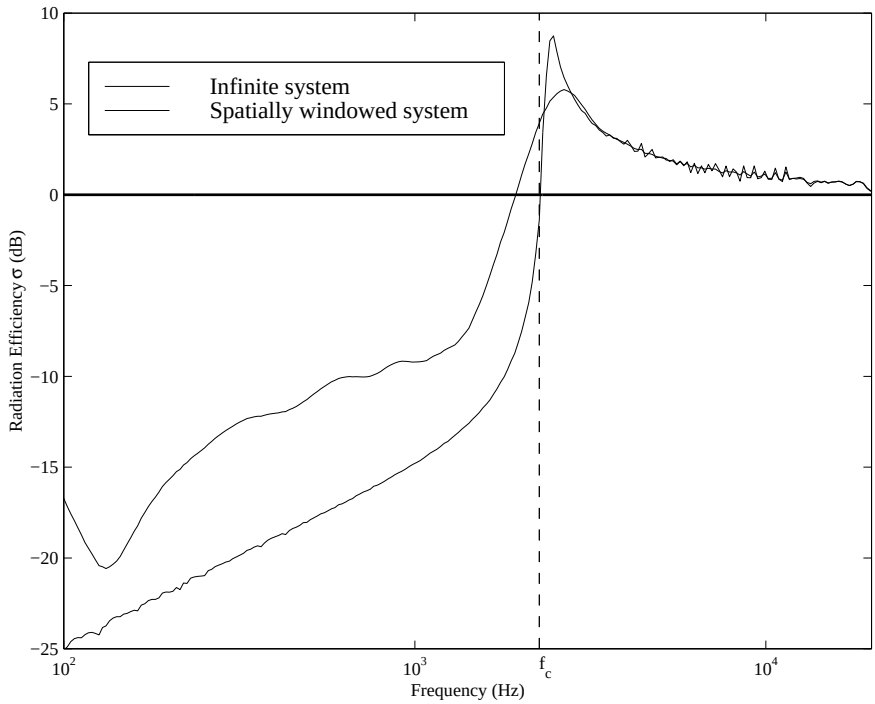

Figure 12: Radiation efficiency of an infinite structure excited by a point force, before and after applying the spatial windowing technique.

Note that the position of the point force is taken into account by the windowing technique. At the limit, the point force can be located out of the spatial window chosen in order to cancel the near field effect ; in this case, the radiation efficiency obtained is, as expected, very close (see figure 13) to the one calculated in section 2.2 for single travelling waves (no excitation) and lower than the one with near field (point force in the middle of the window) .

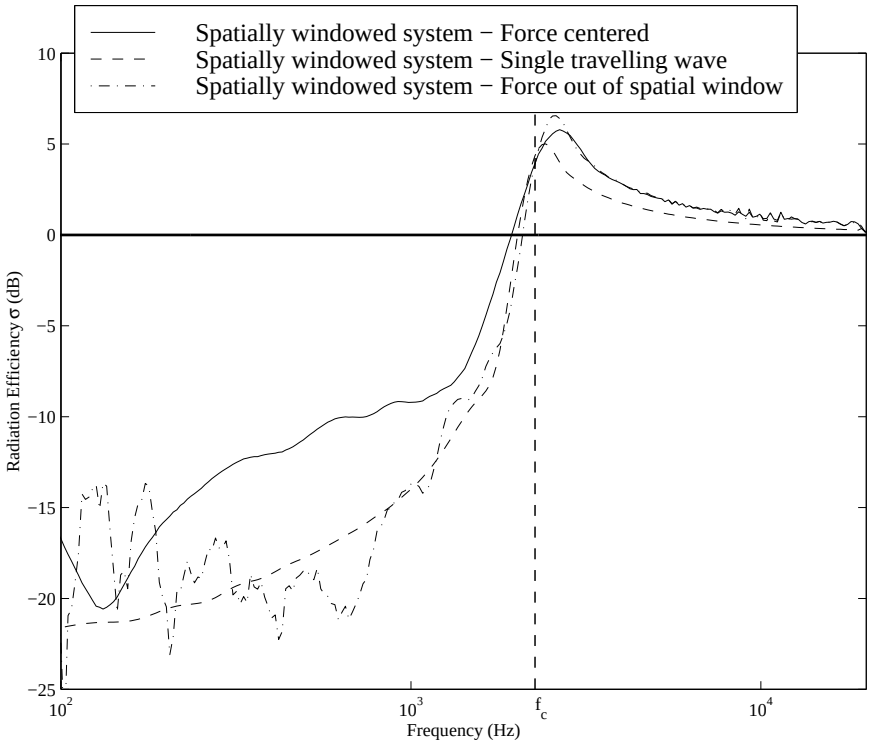

Figure 13: Radiation efficiency of a spatially windowed infinite structure excited by a point force – Force position effect.

2.4.2. Acoustical power radiated

The acoustical power radiated for a given excitation point force, can be written from equation 23 as:

$$\Pi_{\text{finite}}(\omega) = \sigma_{\text{finite}}(\omega)\rho_a c_a S\left\langle v^2 \right\rangle \tag{24}$$

Note that for a real finite structure, the product $S < v^2 >$ would be calculated as

$$S < v^2 >= \frac{1}{2}\iint_S \left|v(x,y)\right|^2 dxdy \tag{25}$$

and represents the vibrational energy stored in the structure. When spatially windowing an infinite structure, the entire infinite structure vibrates and the energy stored must be written according to Parseval's theorem as

$$S\left\langle v^2 \right\rangle = \frac{1}{4\pi^2}\frac{1}{2}\int_{-\infty}^{+\infty}\int_{-\infty}^{+\infty}\left|\tilde{v}_{inf}(k_x,k_y)\right|^2 dk_x\, dk_y \qquad (26)$$

The acoustical power radiated can then be estimated using equations (24) and (26).

3. EXPERIMENTAL VALIDATION

In this section, some results obtained using the spatial windowing technique are presented and compared to experimental results.

3.1. Sound reduction index

3.1.1.Aluminum plate

The case of an aluminum plate, which characteristics are given in Table I, is first considered. First, the sound reduction index is calculated for the infinite plate under a diffuse incident field ($0° \leq \theta \leq 90°$). Then, the diffuseness of the acoustic field incident in the infinite structure is reduced, as usually done by researchers [3, 4, 5] in order to better match computed and measured sound reduction index ; the limiting angle is usually taken to be between 70° and 85° (instead of 90°). Finally, the spatial windowing technique is applied to consider a plate of dimensions 1.1x1.4 m^2. Figure 14 presents these results as well as the corresponding measured ones in third octave bands. The sound reduction index for the infinite structure is much lower (by about 6 dB) than the measured one, but the slope of R is well respected (except at low frequencies). The result of reducing the incident field diffuseness ($0° \leq \theta \leq 70°$) allows to achieve very good agreement with the measurements in the high frequency region (above 1 kHz). However, the slope is not as good as before and the calculated results do not match the measurements in the low frequency range. Using the spatial windowing technique developed in this paper permits a better prediction of the general behavior of the sound reduction index in the low and

high frequency range ; however, it does not permit to predict the modal behavior (see the drop of R at 125 Hz in the measurements) of the finite size plate.

Table I: Material characteristics.

	Aluminum	Glass	Steel	Gypsum Board
Thickness	1.1 mm	4 mm	1 mm	15 mm
Young Modulus	70. GN/m^2	62. GN/m^2	210. GN/m^2	2.5 GN/m^2
Density	2700 kg/m^3	2500 kg/m^3	7850 kg/m^3	690 kg/m^3
Poisson ratio	0.33	0.22	0.3	0.1
Damping	1%	5%	2.0% for $f \leq 250$ Hz 1.5% for 250 Hz $< f \leq 600$ Hz 1.0% for $f \geq 600$ Hz	5%

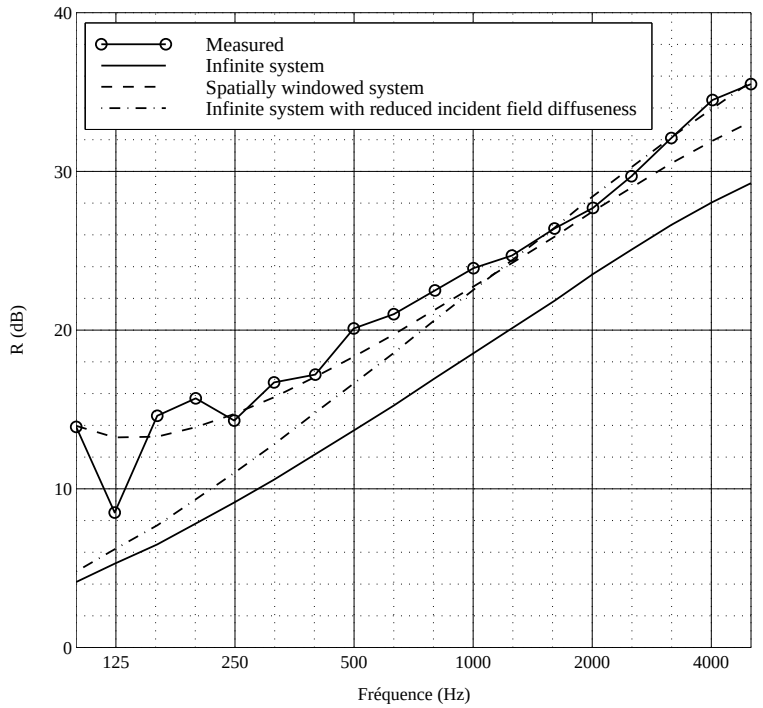

Figure 14 : Sound transmission index for an aluminum plate.

Figure 15 presents the sound reduction index for different sizes of the aluminum plate. As expected, the smallest size plate (0.5 x 0.5 m^2) is associated to the highest transmission index. Increasing the size of the plate to 4.0 x 3.0 m^2 allows the transmission index to get close to that of the infinite structure. The other different sizes of plate considered are associated to a similar surface area and therefore lead to a transmission coefficient of the same order. This demonstrates that this technique does not concentrate on the modal behavior (which would be different for all the different plate dimensions) but rather on the general behavior related to the overall dimensions of the structure.

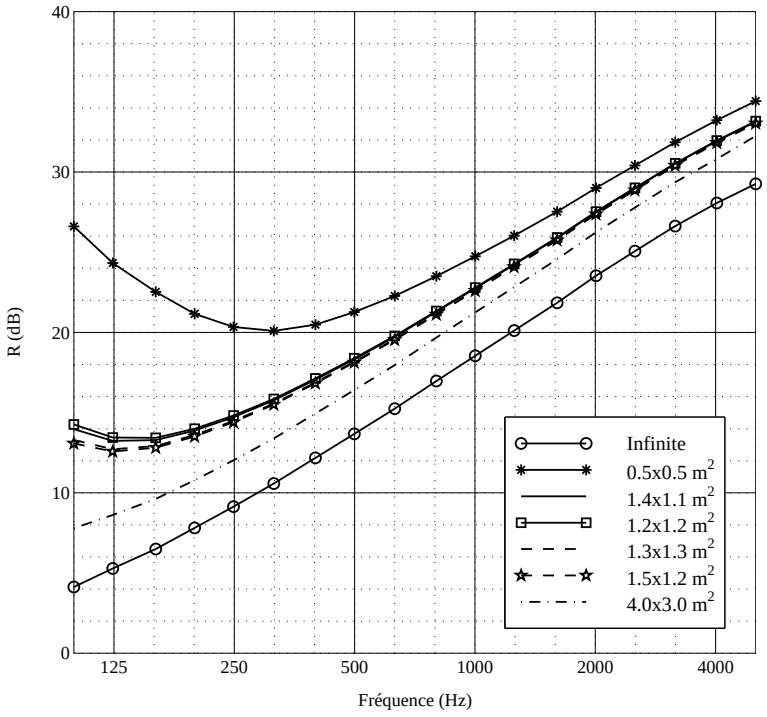

Figure 15 : Sound transmission index for an aluminum plate – Size effect.

3.1.2. Double glazing

The case of a double glazing is now considered. The characteristics of the glass is given in Table I. The air space between the two identical glass panes is 12 mm thick. Figure 16 shows the sound reduction index for the infinite double leaf system, the result of reducing the incident field diffuseness , i.e. $0° \leq \theta \leq 78°$, the result for a glass pane of dimensions 1.48x1.23 m^2 after applying the spatial windowing technique and the measured results. The model of the infinite system fails to predict a transmission index R close to the measured one : it first underestimates the transmission loss over almost the complete frequency range studied, and second it is completely unable to predict the increasing rate of R in the mid frequency range (between 250 and 1000 Hz). The reduction of the incident field diffuseness is associated with a quite spectacular increase of the transmission index between 1 and 2 kHz which does not correspond to any real behavior of the system ; this method is definitely not adapted to the double leaf system considered here. The use of the spatial windowing technique allows as previously to predict a transmission index much closer to the measured one : the general behavior is well respected. An increase of R in the low frequency region (below the cavity resonance frequency at 250 Hz) as seen in the measurements is obtained. Note that a slight difference in the slope between 250 and 1000 Hz still subsists ; this difference could be associated to the encasement of the window in the wall.

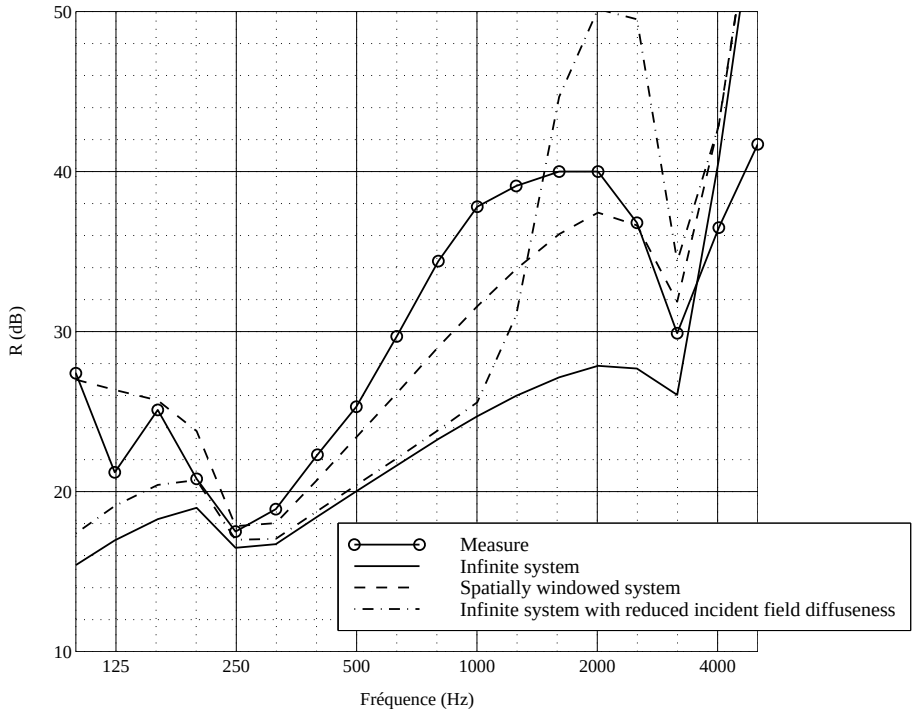

Figure 16 : Sound transmission index for a double window.

Figure 17 presents the sound reduction index for different sizes of the double window. As previously mentioned, the reduction index is similar for dimensions of the double glazing associated to similar surface areas.

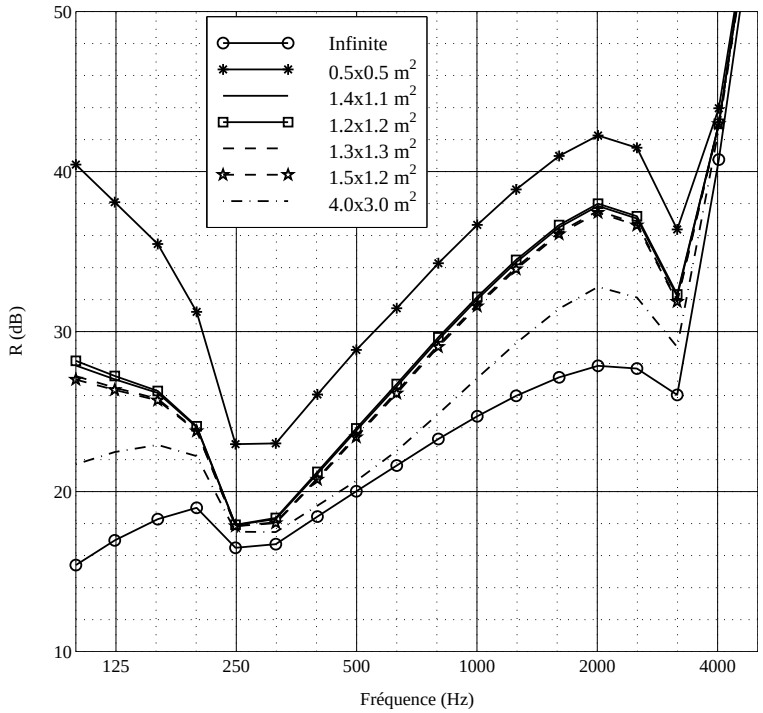

Figure 17 : Sound transmission index for a double window – Size effect.

It has been shown with these two examples, that the use of the spatial windowing technique in the case of acoustical excitation greatly improves the comparison between theory and experiment. The general behavior of the finite structure (if not the modal behavior) in terms of the sound reduction index is well predicted. In the following section, a structural excitation is considered.

3.2. Mechanical excitation (sound radiation)

The case of a steel plate, which characteristics are given in Table I, is now considered. First, the sound radiation efficiency is calculated for the infinite plate under mechanical excitation (point force), then the spatial windowing technique is applied to consider a plate of length 1.3m and width 1.2 m. Figure 18 presents these results as well as the corresponding measured ones in third octave bands (using Nearfield Acoustical Holography [6]). Two point force positions are considered in the calculation : one at the center of the plate and one at the exact position (corresponding to force position during the measurements, i.e., at 0.4 m from the length edge and 0.3 m from the width edge). The radiation efficiency calculated with spatial windowing and the measurements force location is much closer to the measured radiation efficiency than the one calculated without spatial windowing.

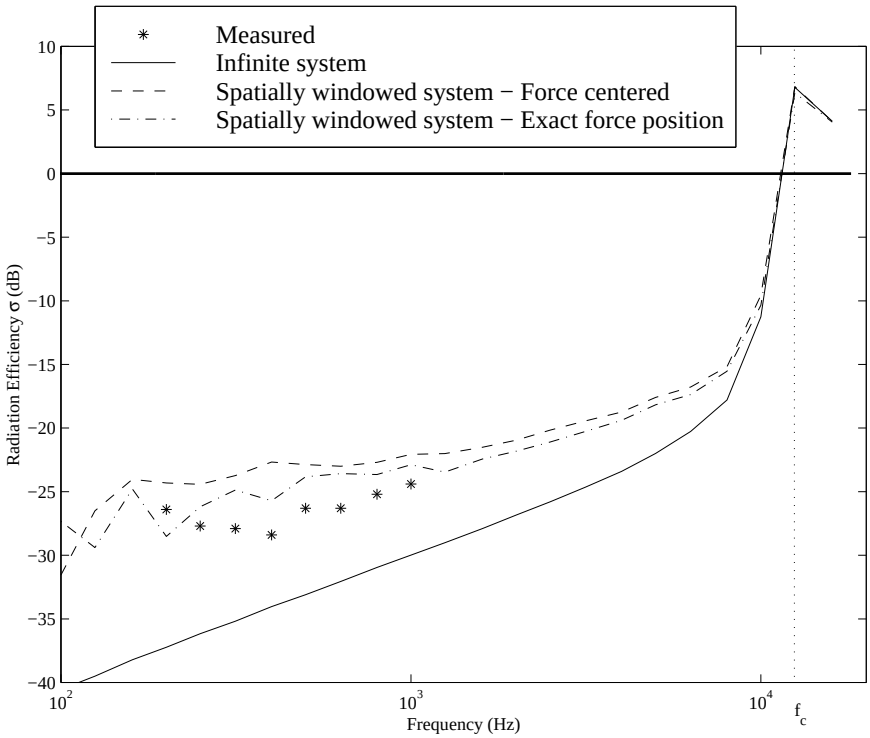

Figure 18 : Sound radiation efficiency for a steel plate.

Figure 20 presents the sound radiated power for different systems introduced for Figure 19. The force level during the measurement was recorded and used to normalize the measured radiated power to an excitation force of 1 N. It can be seen that the radiated power using the spatial windowing technique (and the exact force location) is close to the measured radiated power.

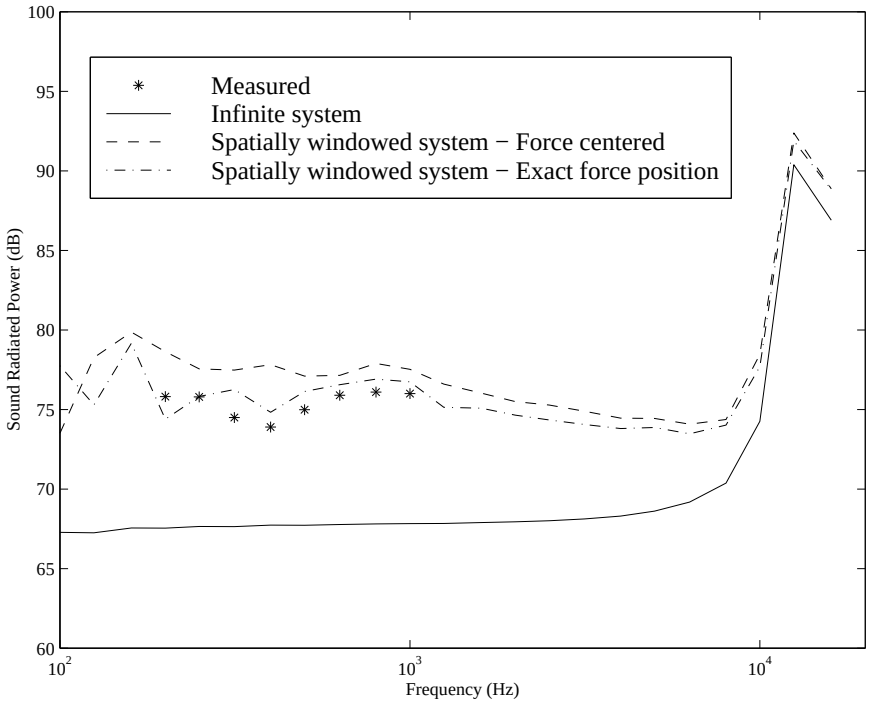

Figure 19 : Sound radiated power for a steel plate.

Figure 20 presents the radiation efficiency for different sizes of the steel plate considered. The excitation force is assumed to be at the center of the plate. As previously mentioned, the radiation efficiency is similar for dimensions of the plate associated to similar surface areas. As the size of the

plate increases to 4.0 x 3.0 m^2, the radiation efficiency of the spatially windowed system approach that of the infinite structure.

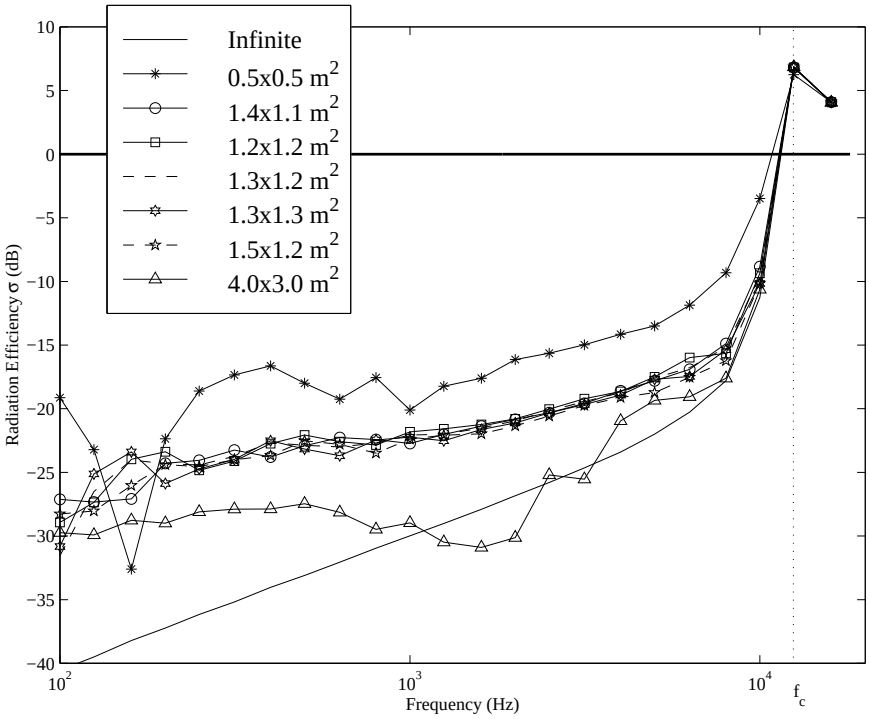

Figure 20 : Sound radiation efficiency for a steel plate – Size effect.

4. CONCLUSIONS

A technique based on a spatial windowing has been presented in order to take the finite size of a plane structure into account without any modal calculations. This technique allows to obtain prediction results much closer to experimental measurements than the classical wave approach applied to infinite structure. Predicted results including the sound transmission index of an aluminum plate and a double leaf window, as well as the radiation efficiency of a metal plate mechanically excited, were presented

and compared to experimental results in order to validate the spatial windowing technique. It was shown that the results (in terms of sound transmission, radiation efficiency, radiated sound power) using spatial windowing were much closer to the measured results than the one calculated without spatial windowing. The effect of the structure size, the size of the spatial window applied to the strucutre, on both its sound transmission (acoustical excitation) and its sound radiation (mechanical excitation) was also discussed.

REFERENCES

1. F. Fahy , *Sound and Structural Vibration , Radiation, Transmission and Response*, Academic Press, London, 1995.

2. M.L. Munjal, "Response of a multi-layered infinite plate to an oblique plane wave by means of transfer matrices", *Journal of Sound and Vibration*, **162**(2), pp. 333-343, 1993.

3. K.A. Mulholland, H.D. Parbrook and A. Cummings, "The transmission loss of double panels", *Journal of Sound and Vibration*, **6**, pp. 324-334, 1967.

4. J.S. Bolton, N.-M. Shiau and Y.K. Kang, "Sound transmission through multi-panel structures lined with elastic porous materials", *Journal of Sound and Vibration*, **191**(3), pp. 317-347, 1996.

5. B. Brouard, D. Lafarge and J.-F. Allard, "A general method of modeling sound propagation in layered media", *Journal of Sound and Vibration*, **183**(1), pp. 129-142, 1995.

6. M. Villot, G. Chavériat and J. Roland, "Phonoscopy : An acoustical holography technique for plane structures radiating in enclosed spaces", *Journal of the Acoustical Society of America*, **91**(1), pp. 187-195, 1992.

View publication stats